

Microstructure and electrochemical properties of rapidly solidified alloy $Ml(NiCoMnTi)_5$

K.Y. Shu^{a,b,*}, X.G. Yang^b, S.K. Zhang^b, G.L. Lü^c, Y.Q. Lei^b, Q.D. Wang^b

^aShanghai Institute of Metallurgy, Chinese Academy of Science, Shanghai 200050, PR China

^bDepartment of Materials Science and Engineering, Zhejiang University, Hangzhou 310027, PR China

^cCenter Laboratory, Zhejiang University, Hangzhou 310028, PR China

Received 27 December 1999; received in revised form 12 September 2000; accepted 9 October 2000

Abstract

The microstructure and electrochemical properties of $MlNi_{3.7}Co_{0.75}Mn_{0.5}Ti_{0.05}$ alloys prepared by both rapid solidification and conventional cast methods were comparatively investigated. SEM and XRD studies showed that the microstructure of conventional cast alloy cooled slowly from its melt was of dendrite, where obvious segregation of Mn and trace second phase $TiNi_3$ were found. However, the rapidly solidified alloy (cooling at a rate of about 10^6 K s^{-1}) was found to be in columnar structure, and contained $CaCu_5$ type single phase only, Mn segregation was restrained effectively as well. Electrochemical measurements showed that the rapidly solidified alloy had higher discharge capacity, more flat discharge potential plateau and longer cycle life than conventional cast alloy, but its activation process was longer. The improved cyclic stability of rapidly solidified alloy was attributed to its composition homogeneity and the fine columnar structure, which showed a good resistance to pulverization and corrosion during charging/discharging cycles. © 2001 Elsevier Science B.V. All rights reserved.

Keywords: Melt-spinning; Electrochemical properties; Composition segregation; Dendrite; Columnar structure

1. Introduction

Ni/MH batteries have developed rapidly recent years for their high discharge capacity and without poisonous element Cd. Among all investigated hydride electrode alloys, AB_5 type mischmetal based alloys have been widely used in making practical Ni/MH batteries due to their good performance–price ratio. As all known the electrochemical properties of the hydride electrode alloys can be greatly improved by selecting the optimum composition of mischmetal in A side and multiple alloying in B side [1]. However, the properties of the alloy is closely related to microstructure which is determined by both composition and material processing. It is increasingly paid attention to the control the microstructure to improve the electrochemical properties of the alloy by changing the solidification mode. The investigation results showed that the cycle stability of the alloy prepared by melt-spinning [2–5], atomization [6,7] and unidirectional solidification [8] was further improved. Rapid solidification, as a new technology for making hydrogen storage alloy, has displayed good prospects in developing

and application of the hydride electrode alloys. In view of the lack of knowledge on the relationship among solidification mode, microstructure and electrochemical properties, it needs further investigation. For the above reasons, microstructure and electrochemical properties of the alloys $Ml(NiCoMnTi)_5$ prepared by both rapid solidification and conventional cast methods were systematically investigated and the relationship between them was also discussed in this paper, where Ml is La-rich mischmetal. The results showed that the reasons causing the change of electrochemical properties were fine columnar structure, single phase and homogeneously distributed component in the rapidly solidified alloy.

2. Experimental details

The alloy with a composition of $MlNi_{3.7}Co_{0.75}Mn_{0.5}Ti_{0.05}$ (simplified as $Ml(NiCoMnTi)_5$ in rest of the paper) was prepared by arc melt under argon atmosphere in a vacuum levitation furnace with water cooled copper crucible. The cooling rate of the alloy in the copper crucible was about 10^2 K s^{-1} . The alloy prepared by above process called as conventional cast (CC) alloy. To ensure the uniformity of the

* Corresponding author. Fax: +86-21-62254273.
E-mail address: sky@itsvr.sim.ac.cn (K.Y. Shu).

alloy, it was turned over and remelted two times. The lanthanum rich mischmetal (MI) composition is as follows: 42 wt.% La, 11 wt.% Ce, 13 wt.% Pr, and 34 wt.% Nd. The purity of the all metals used in alloy melting is higher than 99.95%. Rapidly solidified alloy (or RS alloy) ribbons with thickness about 65 μm were prepared by melt-spinning (rapid solidification) method, and its cooling rate was estimated about 10^6 K s^{-1} according to reference [9].

Both alloys prepared by conventional cast and rapid solidification methods were mechanically grounded into powders below 300 mesh for preparing electrodes and samples in XRD and PCT experiment. About 100 mg alloy powder were mixed with 200 mg copper powder uniformly and then pressed into pellet electrode. Electrochemical properties were tested in a standard trielectrode electroanalysis cell open to the atmosphere. A nickel plate was used as the counter electrode and potentials were referred to an $\text{Hg}/\text{HgO}/\text{OH}^-$. The testing temperature was 25°C . The electrodes were charged at 100 mA g^{-1} for 4 h, then discharge at the current of 50 mA g^{-1} . The discharge cut off potential was set at -0.6 V . Electrolyte was a 6 M KOH solution. The PCT curves were measured with an automatic Sievert's-type apparatus at 298 K. The microscopic structure was observed and analyzed by scanning electron microscope (SEM). The manganese distribution analysis was examined with EDS. The crystalline characteristics of both alloys were analyzed by XRD with Rietveld method. Rietveld refinement of both alloy samples was performed on PC computer with LS1 Software [10]. The more detail information was introduced in [11].

3. Results and discussion

3.1. Microscopic structure and Mn distribution

Fig. 1 is microscopic structure of $\text{MI}(\text{NiCoMnTi})_5$ prepared by rapid solidification and conventional cast methods

observed on SEM. The results show that the microscopic structure of slowly cooled CC alloy is coarse dendrite and the distance between main trunks is about $50 \mu\text{m}$ (see Fig. 1a). While the microscopic structure of rapidly solidified alloy is very fine columnar structure whose size is about $0.3 \mu\text{m}$ (see Fig. 1b). High cooling rate in solidification of the melt alloy often causes large supercooling and makes the alloy formed fine grain and nano-scale crystallite. The large supercooling will be benefit to the melt alloy to form columnar structure also.

Fig. 2 shows the EDS analytical results of Mn distribution in the CC and RS alloys. EDS scanning line in CC alloy is undulant, which means the segregation of manganese in the alloy (shown in Fig. 2a). However, the EDS scanning line in RS alloy is flat, there is no obvious segregation observed (see Fig. 2b). Above results indicate that rapid solidification process can effectively eliminate the composition segregation in $\text{MI}(\text{NiCoMnTi})_5$. Manganese-bearing AB_5 type alloys usually form dendrite or equi-axis grain only due to the accelerating nucleation effect of manganese [12]. But in the rapidly solidified condition in our research, the cooling rate is as high as 10^6 K s^{-1} . Large temperature gradient is formed in the alloy along the direction of normal line of the copper roller, which restrains the manganese segregation during solidification and promotes to form fine columnar structure also. Above result is in accordance with that in $\text{Lm}(\text{NiCoMnAl})_5$ [13].

3.2. XRD analysis

The results of powder XRD analysis of $\text{MI}(\text{NiCoMnTi})_5$ prepared by conventional cast and rapid solidification methods is shown in Fig. 3. The data of XRD are analyzed with Rietveld method and summarized in Table 1. In RS alloy, there is only CaCu_5 type phase discovered and no amorphous or any other phase appear. However, in the slowly solidified CC alloy, there also exists small amount TiNi_3 phase besides the main phase with CaCu_5 type structure (see

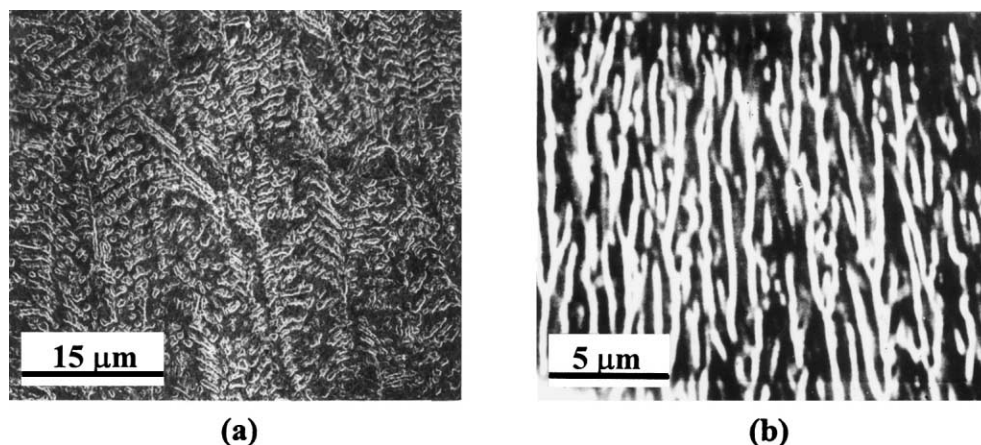


Fig. 1. Microstructure of the alloy $\text{MI}(\text{NiCoMnTi})_5$ prepared by different methods (SEM): (a) conventional cast; (b) melt-spinning (coated by carbon film).

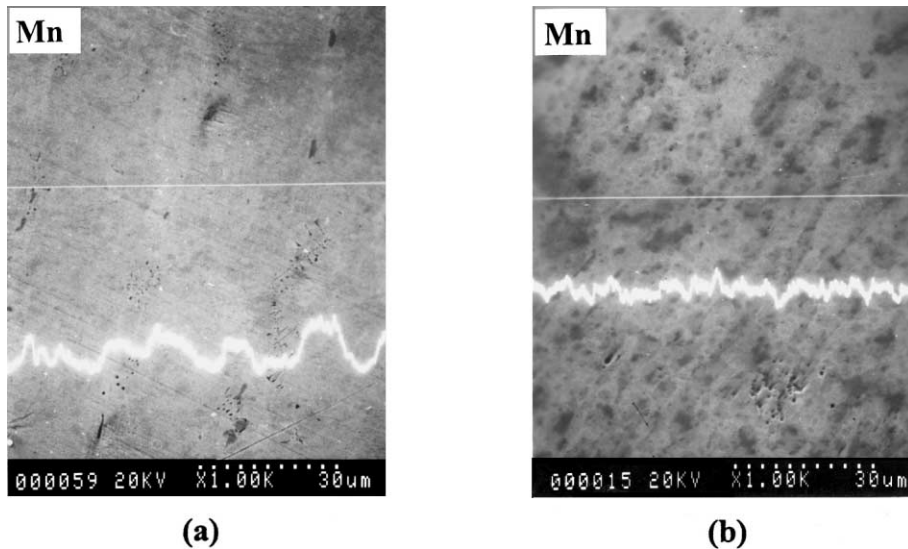


Fig. 2. Manganese distribution in the alloys $Ml(NiCoMnTi)_5$ prepared by (a) conventional cast and (b) melt-spinning.

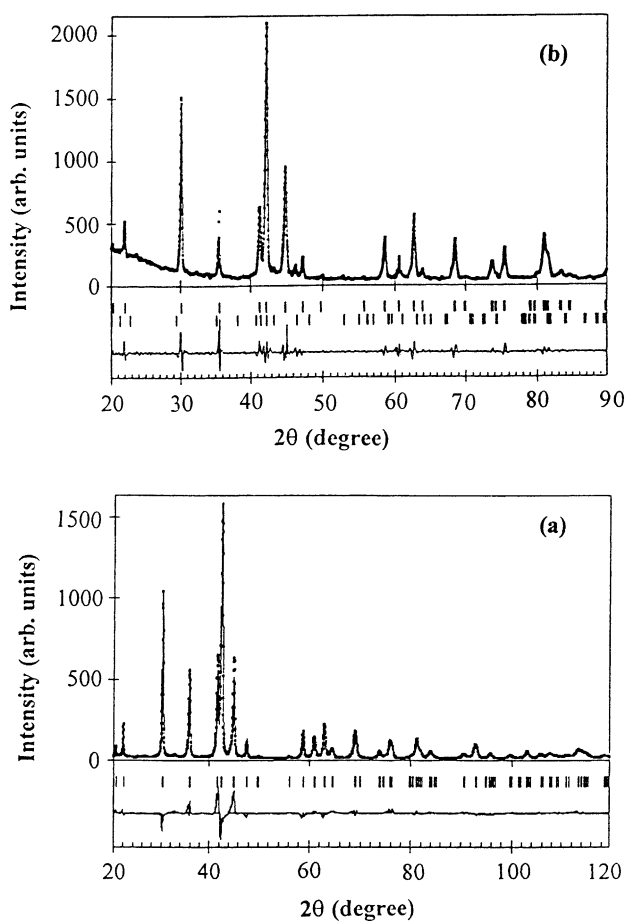


Fig. 3. The X-ray powder diffraction pattern with $Cu K\alpha$ radiation for $Ml(NiCoMnTi)_5$ prepared by (a) rapid solidification and (b) conventional cast. The tick marks below the pattern represent the position of all possible Bragg reflections for $CaCu_5$ type structure and $TiNi_3$.

Fig. 3b). According to the result calculated by Rietveld method (shows in Table 1), there is 2.5 wt.% $TiNi_3$ phase in the CC alloy. Above results show that rapid solidification process could restrain $TiNi_3$ phase to form in $Ml(NiCoMnTi)_5$. Table 1 also indicates the cell parameters and crystallite of both alloys. There is only small difference between the CC alloy and RS alloy on cell parameters.

3.3. Electrochemical properties

3.3.1. Activation and discharge capacity

Fig. 4 shows the activation process of $Ml(NiCoMnTi)_5$ prepared by rapid solidification and conventional cast methods. The activation process of RS alloy is slightly longer than that of CC alloy. The RS alloy needs five cycles to activate and reaches the maximum discharge capacity of 312 mA h g^{-1} , while CC alloy needs only three cycles to activate and reaches the maximum capacity of 302 mA h g^{-1} . The discharge capacity of RS alloy is 10 mA h g^{-1} higher than that of CC alloy. The longer activation cycles of RS alloy is believed concerning to the decrease of crack formed during cycling. The increase of the discharge capacity of RS alloy is ascribed to single phase ($CaCu_5$ type) structure and disappearance of $TiNi_3$ phase that often appears in slowly cooled CC alloy.

3.3.2. High rate dischargeability

Below 1 C discharge current ($1 \text{ C} = 300 \text{ mA g}^{-1}$), the high rate dischargeability (HRD) of both alloys is almost the same, but with the discharge current increase, the CC alloy shows better high rate dischargeability (see Fig. 5). The HRD of hydrogen storage alloy is concerned in electrode reaction dynamics, electrochemical catalytic activity,

Table 1

Cell parameters and phase abundance of the alloys $Mi(NiCoMnTi)_5$ prepared by different methods

Solidification mode	Phase abundance (wt.%)		Cell parameters		
	AB_5	$TiNi_3$	a (nm)	c (nm)	V (nm^3)
Conventional cast	97.5	2.5	0.5003	0.4028	0.0873
Rapid solidification	100	–	0.5006	0.4024	0.0874

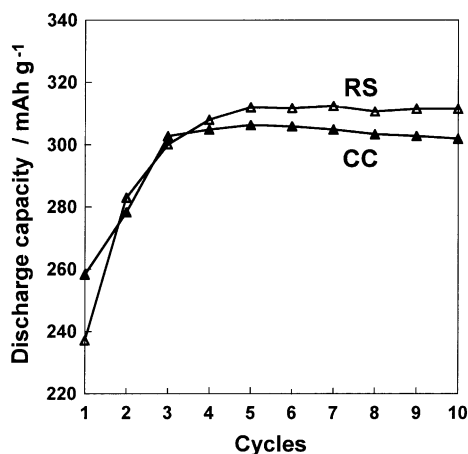
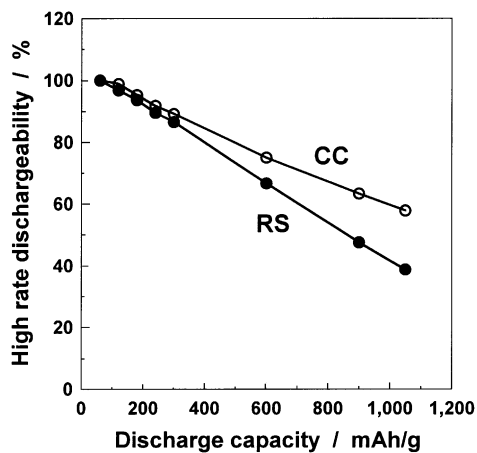
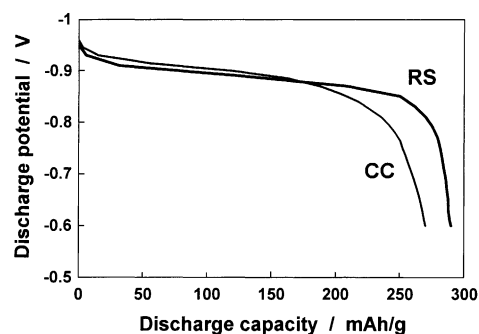


Fig. 4. Activation process of conventional cast and rapidly solidified alloys (298 K).

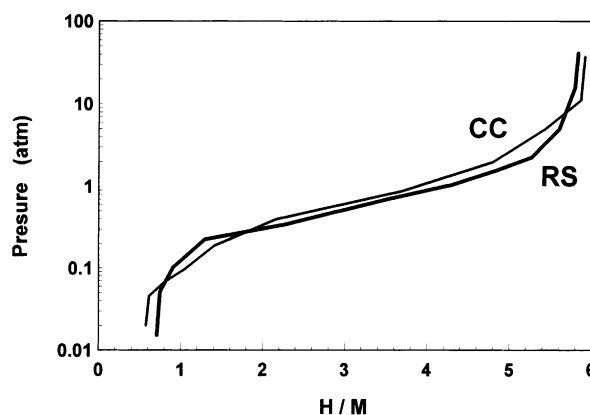
surface area of electrode, hydrogen diffusion velocity and other factors. However, the mechanism affected the high rate dischargeability of rapidly solidified $Mi(NiCoMnTi)_5$ is not clear and further investigation is needed.

3.3.3. PCT curves and discharge potential plateau

It can be seen from discharge curves of both alloys (shown in Fig. 6) that the potential plateau of RS alloy is slightly lower than that of CC alloy, but the plateau of RS alloy is

Fig. 5. High rate dischargeability of $Mi(NiCoMnTi)_5$ prepared by conventional cast and rapid solidification methods at different discharge current (298 K).Fig. 6. Discharge potential curves of the alloys $Mi(NiCoMnTi)_5$ prepared by different methods at discharge current 50 mA g^{-1} (298 K, 50th cycle).

more flat. This is accordance with result of melt-spinning alloy reported early [4]. Fig. 7 shows the PCT curves of both CC and SR alloys. The SR alloy has more flat and wider pressure plateau. The uniformity of the alloy composition is one of the main factors that affect the characteristic of pressure plateau of hydrogen storage alloy. Just as mentioned above, rapid solidification process could effectively restrain the composition segregation and make the composition distribution more uniform, which leads to more flat pressure plateau in PCT curve. The discharge potential plateau is related to the pressure plateau. The flat pressure plateau of hydrogen storage alloy often leads to a flat discharge potential plateau and improves discharge property of hydride electrode and Ni/MH batteries.

Fig. 7. PCT curves for desorption at 298 K for $Mi(NiCoMnTi)_5$ prepared by conventional cast and rapid solidification methods.

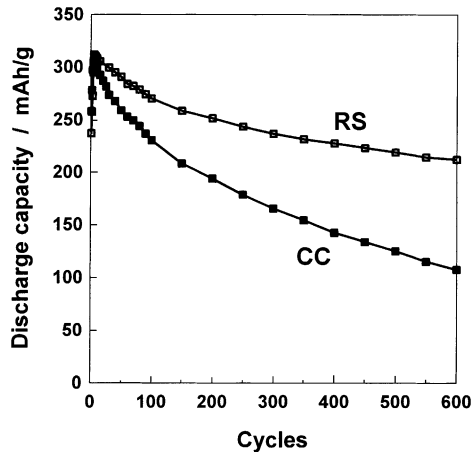


Fig. 8. Cycle stability of conventional cast and rapidly solidified alloys (298 K).

3.3.4. Cycle life

Fig. 8 is long term cycle life of $Ml(NiCoMnTi)_5$ prepared by rapid solidification and conventional cast methods. The result shows that the cycle life of RS alloy is remarkably improved by rapid solidification process. After 600 cycles, the remained capacity of RS alloy is about 70%, while that of CC alloy is below 40%. The cycle stability of hydride electrode is an important property that affects the cycle life of Ni/MH batteries. It is closely related to the rate of pulverization and alloy surface corrosion. The cycle stability remarkably improved is mainly ascribed to fine columnar structure formed in rapid solidification process. As the columnar structure contains a lot of parallel grain boundaries which could release the lattice strain of the alloy caused by absorbing hydrogen, the RS alloy has very good pulverization-resistance. On the other hand, rapid solidification process eliminates the composition segregation in RS alloy and lessens the dissolution rate of component like Mn, La and other elements in cycling, which conduce to raise corrosion-resistance and further improves the cycle stability of the RS alloy.

4. Conclusions

1. The microstructure of slowly cooled conventional cast alloy $Ml(NiCoMnTi)_5$ is coarse dendrite. There obviously exists manganese segregation and $TiNi_3$ secondary phase. However, the microstructure of rapidly solidified alloy is fine columnar structure, the manganese segregation is greatly restrained and $TiNi_3$ phase is completely suppressed.

2. Compared with conventional cast alloy, the cycle stability of rapidly solidified alloy $Ml(NiCoMnTi)_5$ is remarkably improved, but the activation process is slightly prolonged. The electrochemical property change is mainly ascribed to the fine columnar structure that enhances the pulverization-resistance as the alloy absorbing hydrogen. Composition distributed more homogeneous in the rapidly solidified alloy is another reason for prolonging cycle life, which improves corrosion-resistance of the alloy.
3. The discharge capacity of the rapidly solidified alloy is about 10 mA h g^{-1} higher than that of conventional cast alloy because the $TiNi_3$ secondary phase is completely disappeared in rapid solidification process.
4. The high rate dischargeability of rapidly solidified alloy $Ml(NiCoMnTi)_5$ is poorer than that of conventional cast alloy, especially at large discharge current.

Acknowledgements

This work is financially supported by National Advanced Materials Committee and National Natural Science Foundation of China (contracts nos. 59601006 and 59671016).

References

- [1] Y.Q. Lei, J.J. Jiang, D.L. Sun, J. Wu, Q.D. Wang, *J. Alloys Comp.* 231 (1995) 553.
- [2] R. Mishima, H. Miyamura, T. Sakai, N. Kurayama, H. Ishiyama, I. Uehara, *J. Alloys Comp.* 192 (1993) 176.
- [3] Y. Nakamura, H. Nakamura, S. Fujitani, I. Yunezu, *J. Alloys Comp.* 210 (1993) 299.
- [4] W. Tang, G. Sun, *J. Alloys Comp.* 203 (1994) 195.
- [5] C.J. Li, X.L. Wang, *J. Alloys Comp.* 270 (1998) 242, 246.
- [6] A. Züttel, D. Chartouni, K. Gross, P. Spatz, M. Bachler, F. Lichtenberg, A. Fölzer, N.J.E. Adkins, *J. Alloys Comp.* 253/254 (1997) 626.
- [7] F. Lichtenberg, U. Köhler, A. Fölzer, N.J. E Adkins, A. Züttel, *J. Alloys Comp.* 253/254 (1997) 570.
- [8] Y.Q. Lei, Y. Zhou, Y.C. Luo, X.G. Yang, Q.D. Wang, *J. Alloys Comp.* 253/254 (1997) 590.
- [9] H. Jones, *Rep. Prog. Phys.* 36 (1973) 1425.
- [10] L. Lutterotti, R. Scardi, *J. Appl. Cryst.* 25 (1992) 459.
- [11] Kangying Shu, Yongquan Lei, Xiaoguang Yang, Gangfu Lin, Qidong Wang, Guanglie Lü, Linshen Chen, *J. Alloys Comp.* 293–295 (1999) 756.
- [12] T. Sakai, H. Yoshinaga, H. Miyamura, H. Ishikawa, *J. Alloys Comp.* 180 (1992) 37.
- [13] H. Hasebe, Y. Isozaki, M. Kanda, Abstract Booklet of 34th Battery Symposium in Japan, 2C08, 1993, p. 235.